Protein-modified CuS nanotriangles for dual-modal photoacoustic and magnetic resonance imaging

Zhen Yuan, Duyang Gao

Zhen Yuan, Duyang Gao, "Protein-modified CuS nanotriangles for dual-modal photoacoustic and magnetic resonance imaging," Proc. SPIE 11254, Nanoscale Imaging, Sensing, and Actuation for Biomedical Applications XVII, 112540K (21 February 2020); doi: 10.1117/12.2542233

SPIE.

Event: SPIE BiOS, 2020, San Francisco, California, United States

Protein-modified CuS nanotriangles for dual-modal photoacoustic and magnetic resonance imaging

Zhen Yuan, Duyang Gao

Faculty of Health Sciences, University of Macau, Macau SAR, China

Abstract

Controllable preparation of water-soluble multifunctional nanoprobes is of great significance for cancer early diagnosis. In this study, protein-modified hydrophilic copper sufide (CuS) nanotriangles with tunable absorption in the second near-infrared region are developed in the presence of halide ions. Further, DTPA-Gd3+ is conjugated on it by using the unique characteristics of the protein-protected nanotriangles. Specifically, the as-obtained nanostructures are investigated as contrast agents for enhanced in vivo photoacoustic/magnetic resonance dual-modal tumor imaging. More importantly, in vitro and in vivo toxicity analysis are also performed, which show that the dual-modal nanoprobes are biocompatible for most of the cases. It is demonstrated that the novel as-prepared protein-modified nanotriangles are able to work as a nanoplatform to construct dual-modal nanoprobes, which paves a new anenue for improving the photoacoustic/magnetic resonance imaging contrast in cancer detection. It should be pointed out that other functional blocks may also be linked on it, which makes it a general method to design multifunctional nanoprobes.

Keywords: Protein-modified, CuS nanotriangle, photoacoustic imaging, magnetic resonance imaging, dual-modal nanoprobe

*Corresponding author: Prof. Zhen Yuan, Faculty of Health Sciences, University of Macau; Email: zhenyuan@um.edu.mo

Nanoscale Imaging, Sensing, and Actuation for Biomedical Applications XVII, edited by Dror Fixler, Ewa M. Goldys, Proc. of SPIE Vol. 11254, 112540K · © 2020 SPIE
CCC code: 1605-7422/20/$21 · doi: 10.1117/12.2542233

I Introduction

Multimodality imaging has received extensive attention in the past decade because it can take advantages of the complementary structural and functional information from each of the imaging approches.[1] Among all of the available imaging modalities, magnetic resonance imaging (MRI), as a non-invasive technique, has been widely applied in clinic due to its excellent spatial resolution.[2] However, the low sensitivity of MRI limits its applications in monitoring small tissue lesions. In contrast, photoacoustic imaging (PAI), a new hybrid imaging method based upon photoacoustic effect, combining optical and ultrasound properties, not only offers unprecedented advantages of the high sensitivity of optical imaging but also provides the good penetration depth of acoustic imaging.[3] One key way for PAI to readily be integrated into medicine is as an "add-on" to presently accepted high-resolution in vivo imaging systems, such as MRI. Consequently, it is essential to develop new imaging technique that can combibe MRI with PAI, which can detect small tissue structures as well as high resolution and deep tissue penetration. It will play considerable roles in cancer early diagnosis and personalized treatment guidance.

In this study, we established a facile procedure for the colloidal synthesis of water-dispersible triangular CuS nanostructures based on a protein-assisted method. The as-prepared triangular CuS nanostructures were identified to possess several advantages: i) water-soluble and excellent biocompatible; ii) good stability and small size; and iii) easy to be functionalized. In particular, as an ideal contrast agent for PAI, the triangular CuS nanostructures exhibited a tunable absorption covered the second NIR "biological widow" (950 nm- 1300 nm), in which laser possessed its maximum depth of penetration in tissue. More importantly, the protein involved as the capping ligands was revealed to have rich reaction groups including carboxyl groups and amine groups, which made the as-prepared nanostructures a good platform to conjugate functional blocks.[4] In addition, as a proof of concept, gadolinium ions chelating in diethylenetriaminepentaacetic acid (DTPA-Gd^{3+}), a widely used commercialized MRI contrast agent, was adopted for the present work. Consequently, DTPA-Gd^{3+} was linked on the CuS nanostructure easily through reaction between amine group of the protein and carboxyl group of the DTPA, which was activated by 1-Ethyl-3-(3-dimethylaminopropyl)-carbodiimide / N-hydroxysulfosuccinimide (EDC/NHS) chemistry. The DTPA-Gd^{3+}-functionalized CuS NPs, as multimodality imaging probes were carefully characterized, and then successfully applied to PAI/MRI dual-modal imaging in a subcutaneous tumor mice model for in vivo tests. Consequently, we introduce a promising and robust method to construct the new PAI/MRI dual-modal nanoprobes, which can also involve other interesting functional blocks to design multifunctional nanostructures.

II Materials and methods

2.1. Synthesis and Characterization of CuS Nanotriangles

Bovine serum albumin (BSA)-modified CuS triangular nanostructures with good water solubility were facilely prepared in aqueous solution as described in the experiment part. Representative transmission electron microscopy (TEM) (**Figure 1**a) image revealed that the as-prepared BSA-modified CuS nanostructures were monodisperse with an overall diameter of ~14 nm, which were further validated by the findings from high-resolution TEM (HRTEM) (**Figure S1**). A hydrodynamic diameter of 17.52 nm and a negative zeta potential of about 50 mV (insert in Figure 1a) were obtained with the usage of dynamic

light scattering (DLS) analysis, which indicated the as-obtained CuS nanostructures dispersed well in aqueous solution. The large zeta potential also exhibited that BSA as a capping agent, could maintain the aqueous solubility and colloidal stability of the CuS nanostructures. As displayed in Figure S1, the HRTEM image of BSA-modified CuS nanostructures revealed that a triangular shape was generated with well-resolved lattice fringes, demonstrating the highly crystalline nature of the as-prepared NPs. The absorption spectrum of the BSA-modified CuS nanostructures was measured and provided in Figure 1b. Interestingly, it was observed that the absorbance of the nanostructure was above zero over the range of wavelength probed. The as-prepared BSA-modified CuS nanostructures had a broad optical absorption band from 650 nm to 1300 nm with a characterized peak at about 1100 nm. Interesingly, the broad absorption band was able to cover both the NIR I (650 nm - 950 nm) and NIR II (1000 nm - 1350 nm) regions. [5] More importantly, the broad absorption spectrum fit well with the most common wavelengths of lasers used for PAI. In addition, the aqueous solution of the obtained CuS nanostructures manifested a transparent green color (insert in Figure 1b), indicative of well dispersity of BSA-modified CuS nanostructures in water, which was also consistent with the DLS results. It was an important property for biological applications. Further, X-ray photoelectron spectroscopy (XPS) was perfromed to measure the binding energies of BSA-modified CuS nanostructures. As shown in the Cu 2p spectrum (Figure 1c), two peaks at 933.4 eV and 953.8 eV corresponding to Cu(II) $2p_{3/2}$ and Cu(II) $2p_{1/2}$ were identified, which were essentially identical binding energies for the Cu 2p orbital in accordance with Cu^{2+} as reported in the previous references.[6] The crystalline structure of the as-synthesized BSA-modified CuS nanostructures was characterized by using powder X-ray diffraction (XRD). As displayed in Figure 1d, the crystal structure of CuS can be assigned as a typical covellite structure with the existence of strong characteristic (004), (101), (102), (103), (110) and (202) peaks. These observations were consistent well with the findings from the standard spectra of CuS of different lattices, which were also plotted with vertical lines in Figure 1d (JCPDS Card No. 75-2236). The optical properties of the as-obtained BSA-modified triangular CuS nanostructures may be affected by different experiment variables, such as ratio of the copper/sulfur element, amounts of NaOH, the reaction time and the temperature. Ultraviolet-visible-near infrared (UV-Vis-NIR) absorption spectra were recorded to examine the influeces of these experiemntal parameters. The characteristic absorbance peak was shifted from over 1300 nm to 1000 nm with increment of adding S element (**Figure 2**a), which agreed well with our previous work. The blue-shift with increased S ratio was mainly due to the presence of excess S elements which were identified to have weak oxidability.[7] As the oxidation proceeded, an increasing amounts of vacancies were produced and the induced increasement in free carrier concentration can lead to a blue shift of the absorbance peak. Likewise, absorption spetra of CuS nanostructures which were synthesized underling the different concentrations of NaOH were also measured. As shown in Figure 2b, it was observed that the absorbance peak almost showed no differences across the whole absorption band. However, the as-obtained CuS nanostructures which was prepared under low NaOH concentrations (0 mol L^{-1} and 0.04 mol L^{-1}) were found not to stay stable and could precipitate quickly under ambient conditions. The reason was that the BSA molecules can absorb metal ions and entrappe them underling the basic environment, which was also utilized to stabilize other namomaterials as previous report.[8] The absorbance of the as-prepared CuS nanostructures increased gradually with the prolonged

reaction time. It became stable after 50 minutes (Figure 2c). Specifically, the position of the characterized peak was a little blue-shifted. As demonstrated in Figure 2d, a dramatic increase of the BSA-modified CuS absorbance was observed when we changed the reaction temperature. No absorption peaks of the CuS solutions were identified when the reaction happened at 20 °C and 37 °C whereas strong optical absorption were able to be observed after the reaction processed at 70 °C and 90 °C. These observations indicated that higher temperatrure facilitated the formation of CuS nanostructures.

2.2. Stability of the Obtained CuS Nanotriangles

The stability of nanoprobes was of great importance for their biomedical applications, such as in vitro and in vivo imaging. Therefore, the stability of the as-synthesized water-soluble BSA-modified CuS nanoprobes was investigated to explore their potential biological applications.

As displayed in **Figure 3**a, the as-prepared BSA-modified CuS nanoprobes aqueous solution exhibited nearly identical absorbance for about one month under ambient environment, which indicated that the as-prepared nanoprobes possessed excellent store stability. In addition, the stability of the as-prepared nanoprobes at different temperatures were also measured. As demonstrated in Figure 3b, there were no distinct differences of the absorbance among these samples when each sample was examined and maintained at 25 °C, 50 °C and 75 °C for 10 minutes, respectively. Likewise, further tests also showed that BSA-modified CuS nanoprobes were also stable in buffers over a broad range of pH values (pH 4−10) (Figure 3c), in which no precipitation or color change of the nanoprobes dispersed in buffer solution can be observed (insert in Figure 3c). We also investigated the tolerance of the BSA-modified CuS nanoprobes against ion strength by adding salt. More specifically, as can be seen from Figure 3d, there was no precipitation of nanoprobes under high concentration of NaCl solution (2 mol L^{-1}) and the as-prepared nanoprobes appeared to be resistant to high ion strength. Therefore, we can deduce from the findings mentioned above that the as-synthesized water-soluble BSA-modified CuS nanoprobes was able to retain excellent stability. It also indicated that BSA was an excellent capping agent to protect nanomaterials.

2.3. Construction of Multimodal Nanoprobes Based on CuS Nanoplatform

Besides the excellent stabilization of the CuS nanotriangles, BSA is also rich of reaction groups, which enables it to be perfect platform to construct the multimodal nanoprobes through linking functional blocks. In this study, a nanoprobe for PAI/MRI dual-modal imaging was engineered through conjugation of DTPA-Gd^{3+} with BSA-protected CuS nanotriangles.

The absorption spectra of the CuS nanotriangles were measured before and after conjugation of DTPA-Gd^{3+}. As demonstrated in **Figure 4**a, the characteristic absorption peak showed no change. To confirm whether the conjugation was successful executed, we further measured the hydrophilic diameter and the zeta potential of the nanotriangular CuS NPs after conjugation of DTPA-Gd^{3+}, which were displayed in Figure 4b. The hydrophilic diameter was 21.52 nm and zeta potential was about 46 mv below zero for DTPA-Gd^{3+}-functionalized BSA-modified CuS NPs, which were a little larger than that of BSA-modified CuS nanotriangles (insert of Figure 1a). These observations illustrated that DTPA-Gd^{3+} was indeed linked on the nanoplatform. It was noted here that the increase of

the zeta potential may be due to the combined effect from both the Gd^{3+} chelating in DTPA and the reacted amine groups on BSA.

To explore the potential capability of the engineered nanoprobe for dual-modal imaging, in vitro PAI and MRI were perfromed for the present work. For the in vitro PAI tests, the phantom materials used consisted of Intralipid as scattering and India ink as absorber with agar powder (1-2%) for solidifying the Intralipid and India ink solution. DTPA-Gd^{3+}-functionalized BSA-modified CuS nanotriangles solutions-containing targets with five different concentrations (0.156 mg mL^{-1}, 0.312 mg mL^{-1}, 0.625 mg mL^{-1}, 1.25 mg mL^{-1}, and 2.5 mg mL^{-1})) were immersed into the phantom. And then the phantom and associated targets were imaged with our PAI system and the reconstructed photoacoustic images were provided in the insert of Figure 4c**.** More importantly, the photoacoustic signals generated by the water-soluble nanotriangles solutions were found to be linearly dependent on their concentration (R^2 = 0.9903) and the linear relationship was kept when the concentration were ranged from 0.156 mg mL^{-1} to 2.5 mg mL^{-1} (Figure 4c). The experiemntal results demonstrated the nanoprobe can be successfully employed for PAI, even with a low concentration.

The in vitro MRI capability of the DTPA-Gd^{3+}-functionalized BSA-modified CuS nanotriangles dispersed in water were also measured. T1-weighted pseudo-color images were generated and provided in insert of Figure 4d clearly, in which the enhanced magnetic resonance signal intensities were identified due to the utilizaiton of the enhanced contrast agent. In addition, the R1 (1/T1) relaxivity at different concentrations (0, 0.0938, 0.188, 0.375, 0.75, 1.5 mM) of Gd^{3+} containing DTPA-Gd^{3+}-functionalized BSA-modified CuS nanotriangles were measured, and plotted against the concentrations. The R1 was determined by calculating the slope of the linear plot of 1/T1 versus Gd^{3+} concentration (Figure 4d). Based on this, the specific relaxivity of DTPA-Gd^{3+}-functionalized BSA-modified CuS nanotriangles was determined as 6.94 $mM^{-1}S^{-1}$. Interestingly, it was found that the relaxivity of DTPA-Gd^{3+}-functionalized BSA-modified CuS nanotriangles was higher than that of DTPA-Gd^{3+}. This variation was probably attributed to the fact that the structure of the nanomaterials can influence the molecular exchange of H_2O. The observation was consistent with the previous finding.[9] In particualr, this relaxivity value also appeared to be higher than that of commercial MR imaging contrast agents such as Gadovist (3.2 $mM^{-1}S^{-1}$), Omniscan (3.3 $mM^{-1}S^{-1}$), Magnevist (3.2 $mM^{-1}S^{-1}$), and so on.[10] It was noted here that the relaxivity measured is was on a per gadolinium ion basis and was expected to be much higher when is on a per NPs basis. These results also suggested that DTPA-Gd^{3+}-functionalized BSA-modified CuS nanotriangles would have significant potential applications as a contrast agent for MRI.

Before the implementation of the in vivo PAI and MRI, the cytotoxicity of the CuS nanotriangles before and after DTPA-Gd^{3+} conjugation were measured with the usage of standard CCK-8 assay. The nanoprobes exhibited no significant cytotoxicity after 12 h and 24 h incubation of the human primary glioblastoma cell line U87 cells (Figure 4e) and human brain microvascular endothelial cells (Figure 4f), even with the high concentration of 1000 μg mL^{-1}. It was also observed from Figure 4e and Figure 4f that there was no obvious difference of cytotoxicity of the nanoprobe before and after linkage of DTPA-Gd^{3+}. These results indicated that DTPA-Gd^{3+}-functionalized BSA-modified CuS nanotriangles possessed excellent biocompatibility and was an adequate candidate for in vivo dual-modal imaging.

2.4. In vivo Dual-Modal Imaging of U87 Bearing-Tumor Mice

To investigate whether the as-prepared DTPA-Gd^{3+}-functionalized BSA-modified CuS nanotriangles could be used for in vivo dual-modal imaging, nude mice with subcutaneous U87 brain tumor xenografts was established as the animal model of tumor. All procedures were performed in compliance with the guidelines on animal research stipulated by the Animal Care and Use Committee at the Shenzhen Institutes of Advanced Technology, Chinese Academic of Sciences and the University of Macau. When the tumor size reached to 100 mm^3 (**Figure 5**c), the nanoprobes with 100 μL at a concentration of 0.5 mg mL^{-1} were injected intravenously into the nude mice as exogenously administered contrast enhancing agents for in vivo dual-modal PAI/MRI. The photoacoustic signals from a cross section of the tumor were measured at different time intervals. As shown in Figure 5a, before nanoprobes injection (0 h), the photoacoustic image exhibited observable photoacoustic signals in the tumor region, which was due to the endogenous contrast of hemoglobin.[3f] After the tail-vein intravenous injection of nanoprobes, the contrast in tumor site was enhanced with the time increasing, which indicated the nanoprobes can reach the tumor location through enhanced permeability retain (EPR) effect.[11] Quantitative results exhibited that photoacoustic signal strength was over 4 times higher than that from the control group at 24 h post-injection (Figure 5d). The protein coating and adequate hydrophilic size favored efficient EPR effect may explain the significant passive targeting and long residence time in tumors. The PAI results demonstrated that the DTPA-Gd^{3+}-functionalized BSA-modified CuS nanotriangles can be used as PAI contrast agents for enhanced in vivo tumor imaging. Besides the application for PA imaging, the DTPA-Gd^{3+}-functionalized BSA-modified CuS nanotriangles may also be adopted as contrast agents for enhanced MRI since the linkage of DTPA-Gd^{3+}.

To assess the MRI contrast performance of the nanoprobe, the MRI experiments were performed using a clinical 3 MR scanner (TIM TRIO, Siemens, Germany) with a small animal coil. The in vivo T1-weighted MR imaging of nude mice with subcutaneous U87 brain tumor xenografts was implemented before and after tail-vein intravenous injection of DTPA-Gd^{3+}-functionalized BSA-modified CuS nanotriangles (Figure 5b). The obviously increase of T1-weighted signals was clearly observed after 6 h post-injection, and kept growing stronger at 12 h and 24 h post-injection. The magnetic resonance signals were also quantified and given in Figure 5e and we found that all the magnetic resonance molecualr imaging results showed good agreement with the in vivo PAI data, which exhibited the similar biodistribution and the high tumor retention. Therefore, the DTPA-Gd^{3+}-functionalized CuS nanotriangles were revealed to have the photoacoustic/magnetic resonance dual-modal in vivo tumor molecualr imaging ability. As plotted in Figure 5, the tumor was clearly identified with high imaging intensity by both PAI and MRI due to the use of the DTPA-Gd^{3+}-functionalized CuS nanotriangles as contrast agent. The boundary between the tumor and the surrounding tissues was also able to be clearly detected after the agent injection compared to that before the injection.

2.5. In vivo Toxicity of the Dual-Modal Nanoprobes

Blood assay and histology analysis were conducted to study the in vivo toxicity of the developed DTPA-Gd^{3+}-functionalized CuS nanotriangles. As a result, we measured all the important parameters in routine blood analysis including number of white blood cells ($WBC^{\#}$), number of neutrophilic granulocyte ($Gran^{\#}$), the concentration of hemoglobin

(HGB), mean corpuscular hemoglobin concentration (MCHC), mean corpuscular volume (MCV), Hematocrit (HCT), mean platelet volume (MPV), and platelet distribution width (PDW). The mentioned detection indexes remained within the normal ranges, which were also comparable to that of the untreated healthy control. These findings suggested that the DTPA-Gd^{3+}-functionalized CuS nanotriangles had no observable effect on the normal function of the blood. The major organ slices including heart, liver, spleen, lung and kidney were selected for further histological analysis. No obvious morphology damage or inflammation was observed in DTPA-Gd^{3+}-functionalized CuS nanotriangles-treated group and control group in H&E staining images (**Figure 6**), indicating the as-prepared dual-modal contrast agents possessed excellent histocompatibility at the dose tested.

III Conclusions

In summary, we described a general method to construct multimodal nanoprobes based on the protein-modified nanoplatform. Triangular BSA-modified CuS nanoprobes with NIR absorption, which can be tuned by changing the ratios of Cu/S, were developed and adopted as the multimodal nanoplatform. The amount of NaOH added in the reaction exhibited little effect on the wavelength of the nanoplatform while it greatly affected its stability. The reaction time and the temperature that played an important role in the generation of the CuS nanostructures, were also optimized. In addition, the BSA-modified CuS nanoplatform exhibited excellent stability underling the ambient environment, broad pH range (4-10), strong ionic strength and even high temperature up to 75 °C. More importantly, DTPA-Gd^{3+} was further chosen to conjugate on the platform to construct a dual-modal nanoprobe with CuS NPs as the agent for contrast-enhanced PAI while DTPA-Gd^{3+} as the agent for contrast-enhanced MRI. In vitro imaging results showed that the dual-modal nanoprobes can effectively increase the contrast levels in both the photoacoustic images and magnetic resonance images. The nanoprobes also exhibited good biocompatibility. Further, the as-prepared nanoprobes were successfully applied to in vivo photoacoustic/magnetic resonance dual-modal tumor imaging and the PAI and MRI results also exhibited the improved imaging acuracy of tumors such as resolution and contrast. Blood assay and histology analysis were also conducted and the results validated that nanoprobes possessed little toxicity. Therefore, a simple method to construct multimodal nanoprobes was proposed by using the unique properties of protein-protected nanostructures. It is expected that this conjugating approach can be extended to prepare other nanostructures, which will allow the protein-modified nanomaterials to be a good nanoplatform for designing multifunctional nanoprobes that involve the molecular imaging for disease diagnosis and personalized treatment guidance.

Acknowledgement

This study was supported by MYRG2019-00082-FHS and MYRG 2018-00081-FHS grants from the University of Macau in Macau, and also funded by The Science and Technology Development Fund, Macau SAR (FDCT 0011/2018/A1 and FDCT 025/2015/A1).

References

[1] D Gao, P Zhang, Y Liu, Z Sheng, H Chen, Yuan, Zhen. Nanoscale **10**, 19742-19748 (2018).
[2] Gao, DY, Sheng, ZH, Liu, YB, Hu, DR, Zhang, J, Zhang, X., Zheng, HR, & Yuan. Advanced Healthcare Materials, 6(1),1601094 adhm.201601094 (2017).
[3] K Chang, D Gao, Y Liu, Q Qi, Yuan, Zhen. Biomater. Sci., 7, 1486-1492 (2019).
[4] Q. Chen, X. Liu, J. Chen, J. Zeng, Z. Cheng, Z. Liu, Adv. Mater., 6820 (2015).
[5] A. M. Smith, M. C. Mancini, S. Nie, Nat. Nanotechnol. 4, 710 (2009).
[6] J. Yu, J. Zhang, S. Liu, J. Phys. Chem. C., 114, 13642 (2010).
[7]I. Kriegel, C. Jiang, J. Rodríguez-Fernández, R. D. Schaller, D. V. Talapin, E. da Como, J. Feldmann, J. Am. Chem. Soc., 134, 1583 (2012).
[8] P. Huang, L. Bao, D. Yang, G. Gao, J. Lin, Z. Li, C. Zhang, D. Cui, Chem. Asian J., 6, 1156 (2011).
[9] J. S. Ananta, B. Godin, R. Sethi, L. Moriggi, X. Liu, R. E. Serda, R. Krishnamurthy, R. Muthupillai, R. D. Bolskar, L. Helm, Nat. Nanotechnol., 5, 815(2010).
[10] M. Rohrer, H. Bauer, J. Mintorovitch, M. Requardt, H. J. Weinmann, Invest. Radiol. 40, 715 (2005).
[11] Q. W. Tian, J. Q. Hu, Y. H. Zhu, R. J. Zou, Z. G. Chen, S. P. Yang, R. W. Li, Q.Q. Su, Y. Han, X. G. Liu, J. Am. Chem. Soc., 135, 8571 (2013).
[12] Y. Liu, H. Jiang, Z. Yuan, Med.Phys. 43, 3987 (2016).

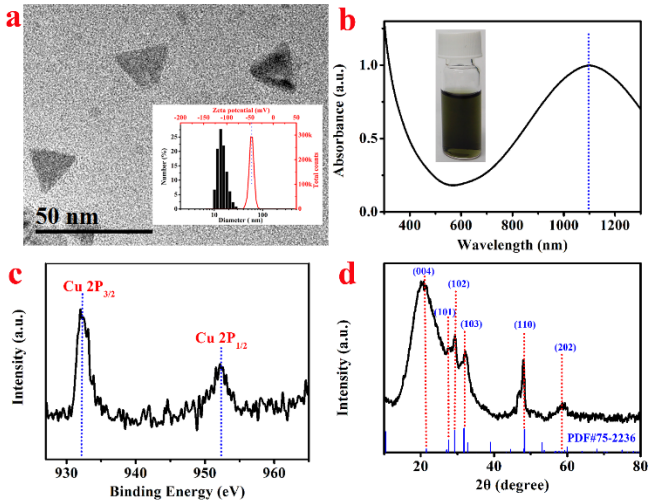

Figure 1. The characterization of the as-prepared CuS nanotriangles. (a) Transmission Electron Micrograph (TEM) image of CuS nanoparticles (NPs) with average size of about 14 nm and insert is zeta potential and diameter measured by dynamic light scattering (DLS) of the NPs dispersed in water; (b) Uv-vis-nir absorption spectrum showing an absorption peak in the near-infrared (NIR) region and photograph under light (insert) of the NPs dispersed in aqueous solution; (c) X-ray Photoelectron Spectroscopy (XPS) spectrum and (d) X-ray diffraction (XRD) data of the as-prepared CuS NPs.

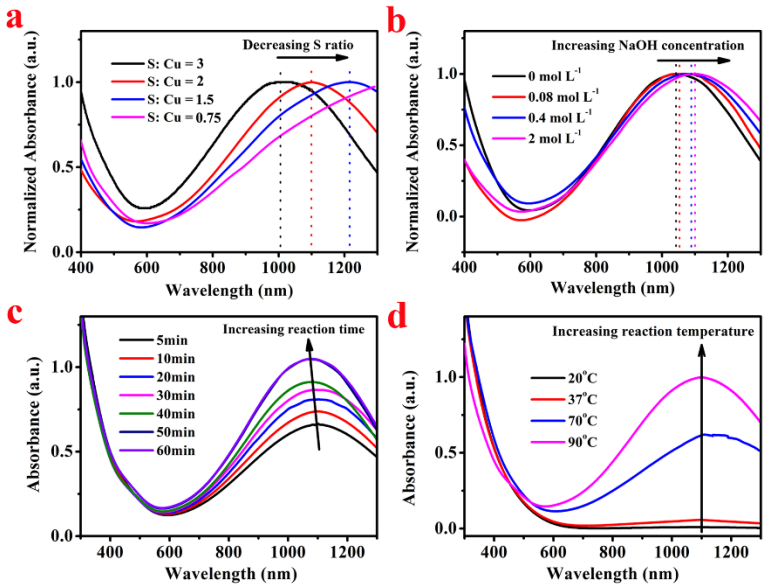

Figure 2. Absorption of the CuS NPs prepared under different conditions. (a) Different ratios of sulfur and copper; (b) different concentrations of NaOH added in the reaction solution; (c) different reaction time; and (d) reaction under different temperature.

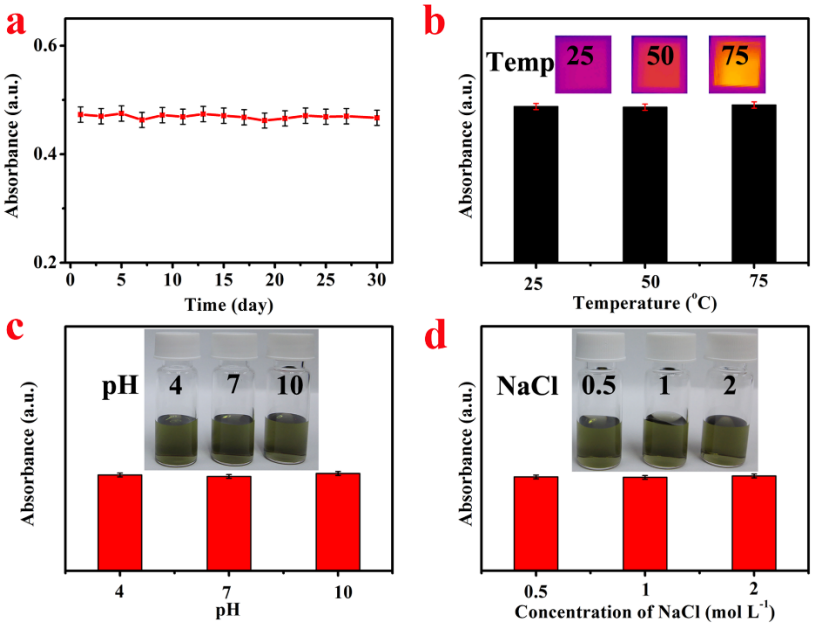

Figure 3. Stability test of the water-soluble CuS NPs. Absorption value at characteristic peak of the CuS NPs stored under room temperature (a), different temperature (Temp 25 °C, 50 °C, and 75 °C) (b), acid, neutral and basic buffer solution (pH 4, 7, and 10) (c), and different concentrations of NaCl (0.5 mol L^{-1}, 1 mol L^{-1}, and 2 mol L^{-1}) (d). The insert of (b) (c) (d) displayed the thermal imaging photograph and photograph under light of the NPs, respectively.

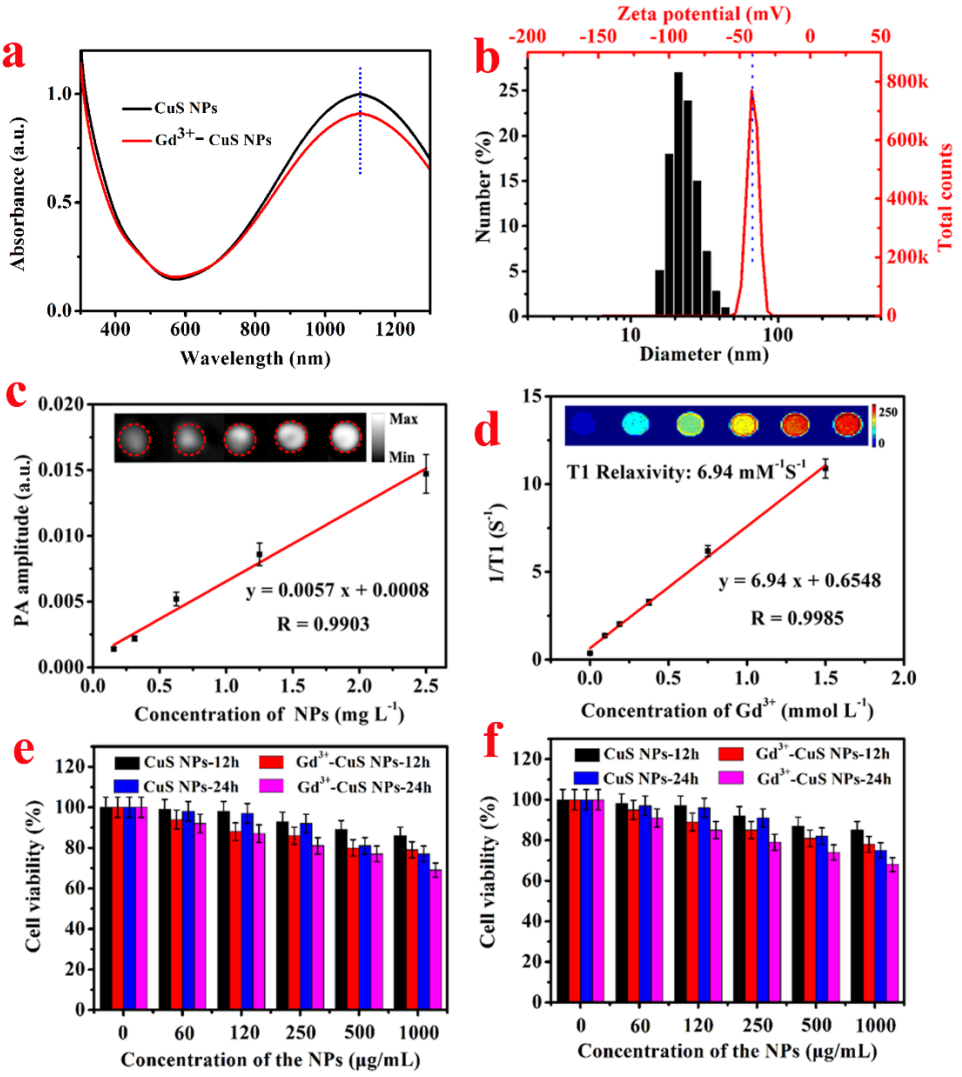

Figure 4. Measurement of Gd^{3+}-functionalized CuS NPs. (a) Absorption spectra of CuS NPs before and after conjugation of DTPA-Gd^{3+}, (b) diameter and zeta potential of the Gd^{3+}-functionalized CuS NPs measured by DLS; (c) photoacoustic images of NPs with different concentrations and the linear relationship between photoacoustic signal intensity and the different concentrations of NPs; (d) T1-weighted MRI contrast images of samples at increasing Gd^{3+} concentrations and plots of 1/T1 (s^{-1}) as a function of Gd^{3+} concentration for the Gd^{3+}-functionalized CuS NPs. The slope indicated the specific relaxivity (6.94 $mM^{-1}S^{-1}$); Cell viability of HBMEC cells (e) and U87 cells (f) recorded after being incubated with CuS NPs before and after conjugation of DTPA-Gd^{3+}.

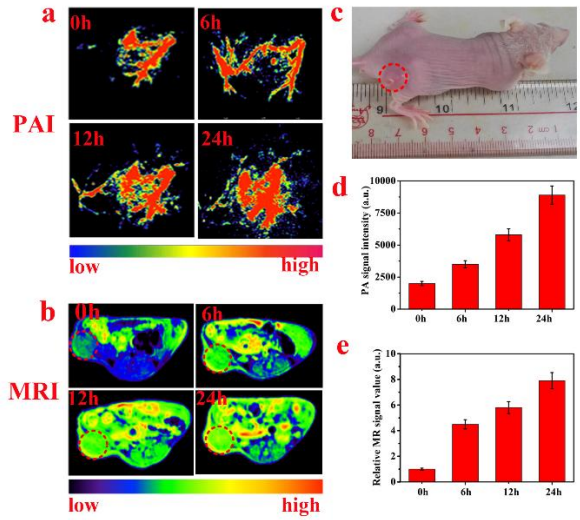

Figure 5. PAI/MRI dual-modal in vivo imaging of the U87 tumor-bearing nude mice. PA images (a) and T1-weighted MRI images (b) before (0h) and at various time points (6 h, 12 h, 24 h) after tail-vein intravenous injection of Gd^{3+}-functionalized CuS NPs, (c) the photograph of U87 subcutaneous tumor-bearing nude mouse; PA (d) and MRI (e) statistical result of the tumor region obtained before (0 h) at 6, 12, and 24 h post tail vein injection of Gd^{3+}-functionalized CuS NPs.

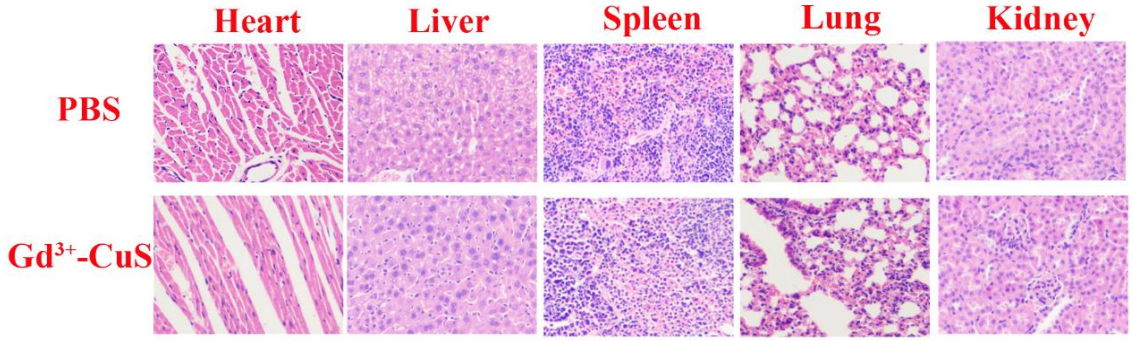

Figure 6. Representative H&E-stained images of major organs including the heart, liver, spleen, kidney, and lung collected from mice sacrificed 7 days after injection of Gd^{3+}-functionalized CuS NPs.